

Study of the decay $D^0 \rightarrow \bar{K}^0 \pi^- e^+ \nu_e$

M. Ablikim,¹ M. N. Achasov,^{10,||} S. Ahmed,¹⁵ M. Albrecht,⁴ M. Alekseyev,^{56a,56c} A. Amoroso,^{56a,56c} F. F. An,¹ Q. An,^{53,42} Y. Bai,⁴¹ O. Bakina,²⁷ R. Baldini Ferroli,^{23a} Y. Ban,³⁵ K. Begzsuren,²⁵ D. W. Bennett,²² J. V. Bennett,⁵ N. Berger,²⁶ M. Bertani,^{23a} D. Bettoni,^{24a} F. Bianchi,^{56a,56c} E. Boger,^{27,‡} I. Boyko,²⁷ R. A. Briere,⁵ H. Cai,⁵⁸ X. Cai,^{1,42} A. Calcaterra,^{23a} G. F. Cao,^{1,46} S. A. Cetin,^{45b} J. Chai,^{56c} J. F. Chang,^{1,42} W. L. Chang,^{1,46} G. Chelkov,^{27,‡,§} G. Chen,¹ H. S. Chen,^{1,46} J. C. Chen,¹ M. L. Chen,^{1,42} P. L. Chen,⁵⁴ S. J. Chen,³³ X. R. Chen,³⁰ Y. B. Chen,^{1,42} W. Cheng,^{56c} X. K. Chu,³⁵ G. Cibinetto,^{24a} F. Cossio,^{56c} H. L. Dai,^{1,42} J. P. Dai,^{37,‡,‡} A. Dbeysi,¹⁵ D. Dedovich,²⁷ Z. Y. Deng,¹ A. Denig,²⁶ I. Denysenko,²⁷ M. Destefanis,^{56a,56c} F. De Mori,^{56a,56c} Y. Ding,³¹ C. Dong,³⁴ J. Dong,^{1,42} L. Y. Dong,^{1,46} M. Y. Dong,^{1,42,46} Z. L. Dou,³³ S. X. Du,⁶¹ P. F. Duan,¹ J. Fang,^{1,42} S. S. Fang,^{1,46} Y. Fang,¹ R. Farinelli,^{24a,24b} L. Fava,^{56b,56c} F. Feldbauer,⁴ G. Felici,^{23a} C. Q. Feng,^{53,42} M. Fritsch,⁴ C. D. Fu,¹ Q. Gao,¹ X. L. Gao,^{53,42} Y. Gao,⁴⁴ Y. G. Gao,⁶ Z. Gao,^{53,42} B. Garillon,²⁶ I. Garzia,^{24a} A. Gilman,⁴⁹ K. Goetzen,¹¹ L. Gong,³⁴ W. X. Gong,^{1,42} W. Gradl,²⁶ M. Greco,^{56a,56c} L. M. Gu,³³ M. H. Gu,^{1,42} Y. T. Gu,¹³ A. Q. Guo,¹ L. B. Guo,³² R. P. Guo,^{1,46} Y. P. Guo,²⁶ A. Guskov,²⁷ Z. Haddadi,²⁹ S. Han,⁵⁸ X. Q. Hao,¹⁶ F. A. Harris,⁴⁷ K. L. He,^{1,46} F. H. Heinsius,⁴ T. Held,⁴ Y. K. Heng,^{1,42,46} Z. L. Hou,¹ H. M. Hu,^{1,46} J. F. Hu,^{37,‡,‡} T. Hu,^{1,42,46} Y. Hu,¹ G. S. Huang,^{53,42} J. S. Huang,¹⁶ X. T. Huang,³⁶ X. Z. Huang,³³ Z. L. Huang,³¹ T. Hussain,⁵⁵ W. Ikegami Andersson,⁵⁷ W. Imoehl,²² M. Irshad,^{53,42} Q. Ji,¹ Q. P. Ji,¹⁶ X. B. Ji,^{1,46} X. L. Ji,^{1,42} H. L. Jiang,³⁶ X. S. Jiang,^{1,42,46} X. Y. Jiang,³⁴ J. B. Jiao,³⁶ Z. Jiao,¹⁸ D. P. Jin,^{1,42,46} S. Jin,³³ Y. Jin,⁴⁸ T. Johansson,⁵⁷ N. Kalantar-Nayestanaki,²⁹ X. S. Kang,³⁴ M. Kavatsyuk,²⁹ B. C. Ke,¹ I. K. Keshk,⁴ T. Khan,^{53,42} A. Khoukaz,⁵⁰ P. Kiese,²⁶ R. Kiuchi,¹ R. Kliemt,¹¹ L. Koch,²⁸ O. B. Kolcu,^{45b,**} B. Kopf,⁴ M. Kuemmel,⁴ M. Kuessner,⁴ A. Kupsc,⁵⁷ M. Kurth,¹ W. Kühn,²⁸ J. S. Lange,²⁸ P. Larin,¹⁵ L. Lavezzi,^{56c} S. Leiber,⁴ H. Leithoff,²⁶ C. Li,⁵⁷ Cheng Li,^{53,42} D. M. Li,⁶¹ F. Li,^{1,42} F. Y. Li,³⁵ G. Li,¹ H. B. Li,^{1,46} H. J. Li,^{1,46} J. C. Li,¹ J. W. Li,⁴⁰ K. J. Li,⁴³ Kang Li,¹⁴ Ke Li,¹ Lei Li,^{3,*} P. L. Li,^{53,42} P. R. Li,^{46,7} Q. Y. Li,³⁶ T. Li,³⁶ W. D. Li,^{1,46} W. G. Li,¹ X. L. Li,³⁶ X. N. Li,^{1,42} X. Q. Li,³⁴ Z. B. Li,⁴³ H. Liang,^{53,42} Y. F. Liang,³⁹ Y. T. Liang,²⁸ G. R. Liao,¹² L. Z. Liao,^{1,46} J. Libby,²¹ C. X. Lin,⁴³ D. X. Lin,¹⁵ B. Liu,^{37,‡,‡} B. J. Liu,¹ C. X. Liu,¹ D. Liu,^{53,42} D. Y. Liu,^{37,‡,‡} F. H. Liu,³⁸ Fang Liu,¹ Feng Liu,⁶ H. B. Liu,¹³ H. L. Liu,⁴¹ H. M. Liu,^{1,46} Huanhuan Liu,¹ Huihui Liu,¹⁷ J. B. Liu,^{53,42} J. Y. Liu,^{1,46} K. Y. Liu,³¹ Ke Liu,⁶ L. D. Liu,³⁵ Q. Liu,⁴⁶ S. B. Liu,^{53,42} X. Liu,³⁰ Y. B. Liu,³⁴ Z. A. Liu,^{1,42,46} Zhiqing Liu,²⁶ Y. F. Long,³⁵ X. C. Lou,^{1,42,46} H. J. Lu,¹⁸ J. G. Lu,^{1,42} Y. Lu,¹ Y. P. Lu,^{1,42} C. L. Luo,³² M. X. Luo,⁶⁰ P. W. Luo,⁴³ T. Luo,^{9,|||} X. L. Luo,^{1,42} S. Lusso,^{56c} X. R. Lyu,⁴⁶ F. C. Ma,³¹ H. L. Ma,¹ L. L. Ma,³⁶ M. M. Ma,^{1,46} Q. M. Ma,¹ X. N. Ma,³⁴ X. Y. Ma,^{1,42} Y. M. Ma,³⁶ F. E. Maas,¹⁵ M. Maggiora,^{56a,56c} S. Maldaner,²⁶ S. Malde,⁵¹ Q. A. Malik,⁵⁵ A. Mangoni,^{23b} Y. J. Mao,³⁵ Z. P. Mao,¹ S. Marcello,^{56a,56c} Z. X. Meng,⁴⁸ J. G. Messchendorp,²⁹ G. Mezzadri,^{24a} J. Min,^{1,42} T. J. Min,³³ R. E. Mitchell,²² X. H. Mo,^{1,42,46} Y. J. Mo,⁶ C. Morales Morales,¹⁵ N. Yu. Muchnoi,^{10,||} H. Muramatsu,⁴⁹ A. Mustafa,⁴ S. Nakhoul,^{11,††} Y. Nefedov,²⁷ F. Nerling,^{11,††} I. B. Nikolaev,^{10,||} Z. Ning,^{1,42} S. Nisar,⁸ S. L. Niu,^{1,42} X. Y. Niu,^{1,46} S. L. Olsen,⁴⁶ Q. Ouyang,^{1,42,46} S. Pacetti,^{23b} Y. Pan,^{53,42} M. Papenbrock,⁵⁷ P. Patteri,^{23a} M. Pelizaeus,⁴ J. Pellegrino,^{56a,56c} H. P. Peng,^{53,42} Z. Y. Peng,¹³ K. Peters,^{11,††} J. Pettersson,⁵⁷ J. L. Ping,³² R. G. Ping,^{1,46} A. Pitka,⁴ R. Poling,⁴⁹ V. Prasad,^{53,42} H. R. Qi,² M. Qi,³³ T. Y. Qi,² S. Qian,^{1,42} C. F. Qiao,⁴⁶ N. Qin,⁵⁸ X. S. Qin,⁴ Z. H. Qin,^{1,42} J. F. Qiu,¹ S. Q. Qu,³⁴ K. H. Rashid,^{55,§§} C. F. Redmer,²⁶ M. Richter,⁴ M. Ripka,²⁶ A. Rivetti,^{56c} M. Rolo,^{56c} G. Rong,^{1,46} Ch. Rosner,¹⁵ A. Sarantsev,^{27,¶} M. Savrić,^{24b} K. Schoenning,⁵⁷ W. Shan,¹⁹ X. Y. Shan,^{53,42} M. Shao,^{53,42} C. P. Shen,² P. X. Shen,³⁴ X. Y. Shen,^{1,46} H. Y. Sheng,¹ X. Shi,^{1,42} J. J. Song,³⁶ W. M. Song,³⁶ X. Y. Song,¹ S. Sosio,^{56a,56c} C. Sowa,⁴ S. Spataro,^{56a,56c} F. F. Sui,³⁶ G. X. Sun,¹ J. F. Sun,¹⁶ L. Sun,⁵⁸ S. S. Sun,^{1,46} X. H. Sun,¹ Y. J. Sun,^{53,42} Y. K. Sun,^{53,42} Y. Z. Sun,¹ Z. J. Sun,^{1,42} Z. T. Sun,¹ Y. T. Tan,^{53,42} C. J. Tang,³⁹ G. Y. Tang,¹ X. Tang,¹ M. Tiemens,²⁹ B. Tsednee,²⁵ I. Uman,^{45d} B. Wang,¹ B. L. Wang,⁴⁶ C. W. Wang,³³ D. Wang,³⁵ D. Y. Wang,³⁵ H. H. Wang,³⁶ K. Wang,^{1,42} L. L. Wang,¹ L. S. Wang,¹ M. Wang,³⁶ Meng Wang,^{1,46} P. Wang,¹ P. L. Wang,¹ W. P. Wang,^{53,42} X. F. Wang,¹ Y. Wang,^{53,42} Y. F. Wang,^{1,42,46} Y. Q. Wang,¹⁶ Z. Wang,^{1,42} Z. G. Wang,^{1,42} Z. Y. Wang,¹ Zongyuan Wang,^{1,46} T. Weber,⁴ D. H. Wei,¹² P. Weidenkaff,²⁶ S. P. Wen,¹ U. Wiedner,⁴ M. Wolke,⁵⁷ L. H. Wu,¹ L. J. Wu,^{1,46} Z. Wu,^{1,42} L. Xia,^{53,42} X. Xia,³⁶ Y. Xia,²⁰ D. Xiao,¹ Y. J. Xiao,^{1,46} Z. J. Xiao,³² Y. G. Xie,^{1,42} Y. H. Xie,⁶ X. A. Xiong,^{1,46} Q. L. Xiu,^{1,42} G. F. Xu,¹ J. J. Xu,^{1,46} L. Xu,¹ Q. J. Xu,¹⁴ X. P. Xu,⁴⁰ F. Yan,⁵⁴ L. Yan,^{56a,56c} W. B. Yan,^{53,42} W. C. Yan,² Y. H. Yan,²⁰ H. J. Yang,^{37,‡,‡} H. X. Yang,¹ L. Yang,⁵⁸ R. X. Yang,^{53,42} S. L. Yang,^{1,46} Y. H. Yang,³³ Y. X. Yang,¹² Yifan Yang,^{1,46} Z. Q. Yang,²⁰ M. Ye,^{1,42} M. H. Ye,⁷ J. H. Yin,¹ Z. Y. You,⁴³ B. X. Yu,^{1,42,46} C. X. Yu,³⁴ J. S. Yu,²⁰ J. S. Yu,³⁰ C. Z. Yuan,^{1,46} Y. Yuan,¹ A. Yuncu,^{45b,†} A. A. Zafar,⁵⁵ Y. Zeng,²⁰ B. X. Zhang,¹ B. Y. Zhang,^{1,42} C. C. Zhang,¹ D. H. Zhang,¹ H. H. Zhang,⁴³ H. Y. Zhang,^{1,42} J. Zhang,^{1,46} J. L. Zhang,⁵⁹ J. Q. Zhang,⁴ J. W. Zhang,^{1,42,46} J. Y. Zhang,¹ J. Z. Zhang,^{1,46} K. Zhang,^{1,46} L. Zhang,⁴⁴ S. F. Zhang,³³ T. J. Zhang,^{37,‡,‡} X. Y. Zhang,³⁶ Y. Zhang,^{53,42} Y. H. Zhang,^{1,42} Y. T. Zhang,^{53,42} Yang Zhang,¹ Yao Zhang,¹ Yu Zhang,⁴⁶ Z. H. Zhang,⁶ Z. P. Zhang,⁵³ Z. Y. Zhang,⁵⁸ G. Zhao,¹ J. W. Zhao,^{1,42} J. Y. Zhao,^{1,46} J. Z. Zhao,^{1,42} Lei Zhao,^{53,42} Ling Zhao,¹ M. G. Zhao,³⁴ Q. Zhao,¹ S. J. Zhao,⁶¹ T. C. Zhao,¹ Y. B. Zhao,^{1,42} Z. G. Zhao,^{53,42} A. Zhemchugov,^{27,‡} B. Zheng,⁵⁴ J. P. Zheng,^{1,42} W. J. Zheng,³⁶ Y. H. Zheng,⁴⁶ B. Zhong,³² L. Zhou,^{1,42} Q. Zhou,^{1,46} X. Zhou,⁵⁸ X. K. Zhou,^{53,42}

X. R. Zhou,^{53,42} X. Y. Zhou,¹ Xiaoyu Zhou,²⁰ Xu Zhou,²⁰ A. N. Zhu,^{1,46} J. Zhu,³⁴ J. Zhu,⁴³ K. Zhu,¹ K. J. Zhu,^{1,42,46} S. Zhu,¹
S. H. Zhu,⁵² X. L. Zhu,⁴⁴ Y. C. Zhu,^{53,42} Y. S. Zhu,^{1,46} Z. A. Zhu,^{1,46} J. Zhuang,^{1,42} B. S. Zou,¹ and J. H. Zou¹

(BESIII Collaboration)

- ¹*Institute of High Energy Physics, Beijing 100049, People's Republic of China*
²*Beihang University, Beijing 100191, People's Republic of China*
³*Beijing Institute of Petrochemical Technology, Beijing 102617, People's Republic of China*
⁴*Bochum Ruhr-University, D-44780 Bochum, Germany*
⁵*Carnegie Mellon University, Pittsburgh, Pennsylvania 15213, USA*
⁶*Central China Normal University, Wuhan 430079, People's Republic of China*
⁷*China Center of Advanced Science and Technology, Beijing 100190, People's Republic of China*
⁸*COMSATS Institute of Information Technology, Lahore, Defence Road, Off Raiwind Road, 54000 Lahore, Pakistan*
⁹*Fudan University, Shanghai 200443, People's Republic of China*
¹⁰*G.I. Budker Institute of Nuclear Physics SB RAS (BINP), Novosibirsk 630090, Russia*
¹¹*GSI Helmholtzcentre for Heavy Ion Research GmbH, D-64291 Darmstadt, Germany*
¹²*Guangxi Normal University, Guilin 541004, People's Republic of China*
¹³*Guangxi University, Nanning 530004, People's Republic of China*
¹⁴*Hangzhou Normal University, Hangzhou 310036, People's Republic of China*
¹⁵*Helmholtz Institute Mainz, Johann-Joachim-Becher-Weg 45, D-55099 Mainz, Germany*
¹⁶*Henan Normal University, Xinxiang 453007, People's Republic of China*
¹⁷*Henan University of Science and Technology, Luoyang 471003, People's Republic of China*
¹⁸*Huangshan College, Huangshan 245000, People's Republic of China*
¹⁹*Hunan Normal University, Changsha 410081, People's Republic of China*
²⁰*Hunan University, Changsha 410082, People's Republic of China*
²¹*Indian Institute of Technology Madras, Chennai 600036, India*
²²*Indiana University, Bloomington, Indiana 47405, USA*
^{23a}*INFN Laboratori Nazionali di Frascati, I-00044, Frascati, Italy*
^{23b}*INFN and University of Perugia, I-06100, Perugia, Italy*
^{24a}*INFN Sezione di Ferrara, I-44122, Ferrara, Italy*
^{24b}*University of Ferrara, I-44122, Ferrara, Italy*
²⁵*Institute of Physics and Technology, Peace Ave. 54B, Ulaanbaatar 13330, Mongolia*
²⁶*Johannes Gutenberg University of Mainz, Johann-Joachim-Becher-Weg 45, D-55099 Mainz, Germany*
²⁷*Joint Institute for Nuclear Research, 141980 Dubna, Moscow region, Russia*
²⁸*Justus-Liebig-Universitaet Giessen, II. Physikalisches Institut, Heinrich-Buff-Ring 16, D-35392 Giessen, Germany*
²⁹*KVI-CART, University of Groningen, NL-9747 AA Groningen, The Netherlands*
³⁰*Lanzhou University, Lanzhou 730000, People's Republic of China*
³¹*Liaoning University, Shenyang 110036, People's Republic of China*
³²*Nanjing Normal University, Nanjing 210023, People's Republic of China*
³³*Nanjing University, Nanjing 210093, People's Republic of China*
³⁴*Nankai University, Tianjin 300071, People's Republic of China*
³⁵*Peking University, Beijing 100871, People's Republic of China*
³⁶*Shandong University, Jinan 250100, People's Republic of China*
³⁷*Shanghai Jiao Tong University, Shanghai 200240, People's Republic of China*
³⁸*Shanxi University, Taiyuan 030006, People's Republic of China*
³⁹*Sichuan University, Chengdu 610064, People's Republic of China*
⁴⁰*Soochow University, Suzhou 215006, People's Republic of China*
⁴¹*Southeast University, Nanjing 211100, People's Republic of China*
⁴²*State Key Laboratory of Particle Detection and Electronics, Beijing 100049, Hefei 230026, People's Republic of China*
⁴³*Sun Yat-Sen University, Guangzhou 510275, People's Republic of China*
⁴⁴*Tsinghua University, Beijing 100084, People's Republic of China*
^{45a}*Ankara University, 06100 Tandogan, Ankara, Turkey*
^{45b}*Istanbul Bilgi University, 34060 Eyup, Istanbul, Turkey*
^{45c}*Uludag University, 16059 Bursa, Turkey*
^{45d}*Near East University, Nicosia, North Cyprus, Mersin 10, Turkey*
⁴⁶*University of Chinese Academy of Sciences, Beijing 100049, People's Republic of China*
⁴⁷*University of Hawaii, Honolulu, Hawaii 96822, USA*

⁴⁸University of Jinan, Jinan 250022, People's Republic of China⁴⁹University of Minnesota, Minneapolis, Minnesota 55455, USA⁵⁰University of Muenster, Wilhelm-Klemm-Str. 9, 48149 Muenster, Germany⁵¹University of Oxford, Keble Road, Oxford OX13RH, United Kingdom⁵²University of Science and Technology Liaoning, Anshan 114051, People's Republic of China⁵³University of Science and Technology of China, Hefei 230026, People's Republic of China⁵⁴University of South China, Hengyang 421001, People's Republic of China⁵⁵University of the Punjab, Lahore-54590, Pakistan^{56a}University of Turin, I-10125, Turin, Italy^{56b}University of Eastern Piedmont, I-15121, Alessandria, Italy^{56c}INFN, I-10125, Turin, Italy⁵⁷Uppsala University, Box 516, SE-75120 Uppsala, Sweden⁵⁸Wuhan University, Wuhan 430072, People's Republic of China⁵⁹Xinyang Normal University, Xinyang 464000, People's Republic of China⁶⁰Zhejiang University, Hangzhou 310027, People's Republic of China⁶¹Zhengzhou University, Zhengzhou 450001, People's Republic of China

(Received 28 November 2018; published 25 January 2019)

We report a study of the decay $D^0 \rightarrow \bar{K}^0 \pi^- e^+ \nu_e$ based on a sample of $2.93 \text{ fb}^{-1} e^+ e^-$ annihilation data collected at the center-of-mass energy of 3.773 GeV with the BESIII detector at the BEPCII collider. The total branching fraction is determined to be $\mathcal{B}(D^0 \rightarrow \bar{K}^0 \pi^- e^+ \nu_e) = (1.434 \pm 0.029(\text{stat.}) \pm 0.032(\text{syst.}))\%$, which is the most precise to date. According to a detailed analysis of the involved dynamics, we find this decay is dominated with the $K^*(892)^-$ contribution and present an improved measurement of its branching fraction to be $\mathcal{B}(D^0 \rightarrow K^*(892)^- e^+ \nu_e) = (2.033 \pm 0.046(\text{stat.}) \pm 0.047(\text{syst.}))\%$. We further access their hadronic form-factor ratios for the first time as $r_V = V(0)/A_1(0) = 1.46 \pm 0.07(\text{stat.}) \pm 0.02(\text{syst.})$ and $r_2 = A_2(0)/A_1(0) = 0.67 \pm 0.06(\text{stat.}) \pm 0.01(\text{syst.})$. In addition, we observe a significant $\bar{K}^0 \pi^- S$ -wave component accounting for $(5.51 \pm 0.97(\text{stat.}) \pm 0.62(\text{syst.}))\%$ of the total decay rate.

DOI: [10.1103/PhysRevD.99.011103](https://doi.org/10.1103/PhysRevD.99.011103)

I. INTRODUCTION

The studies on semileptonic (SL) decay modes of charm mesons provide valuable information on the weak and strong interactions in mesons composed of heavy quarks [1]. The semileptonic partial decay width is related to the product of the hadronic form factor describing the strong-interaction in the initial and final hadrons, and the Cabibbo-Kobayashi-Maskawa (CKM) matrix elements $|V_{cs}|$ and $|V_{cd}|$, which parametrize the mixing between the quark flavors in the weak interaction [2]. The couplings $|V_{cs}|$ and $|V_{cd}|$ are tightly constrained by the unitarity of the CKM matrix. Thus, detailed studies of the dynamics of the SL decays allow measurements of the hadronic form factors, which are important for calibrating the theoretical calculations of the involved strong interaction.

The relative simplicity of theoretical description of the SL decay $D \rightarrow \bar{K} \pi e^+ \nu_e$ [3] makes it a optimal place to study the $\bar{K} \pi$ system, and to further determine the hadronic transition form factors. Measurements of $\bar{K} \pi$ resonant and non-resonant amplitudes in the decay $D^+ \rightarrow K^- \pi^+ e^+ \nu_e$ have been reported by the CLEO [4], BABAR [5] and BESIII [6] collaborations. In these studies a nontrivial S -wave component is observed along with the dominant P -wave one. A study of the dynamics in the isospin-symmetric mode $D^0 \rightarrow \bar{K}^0 \pi^- e^+ \nu_e$ will provide complementary information

*Corresponding author.

lilei2014@bipt.edu.cn

[†]Also at Bogazici University, 34342 Istanbul, Turkey.[‡]Also at the Moscow Institute of Physics and Technology, Moscow 141700, Russia.[§]Also at the Functional Electronics Laboratory, Tomsk State University, Tomsk, 634050, Russia.^{||}Also at the Novosibirsk State University, Novosibirsk, 630090, Russia.[¶]Also at the NRC ‘‘Kurchatov Institute’’, PNPI, 188300, Gatchina, Russia.^{**}Also at Istanbul Arel University, 34295 Istanbul, Turkey.^{††}Also at Goethe University Frankfurt, 60323 Frankfurt am Main, Germany.^{‡‡}Also at Key Laboratory for Particle Physics, Astrophysics and Cosmology, Ministry of Education; Shanghai Key Laboratory for Particle Physics and Cosmology; Institute of Nuclear and Particle Physics, Shanghai 200240, People's Republic of China.^{§§}Also at Government College Women University, Sialkot—51310, Punjab, Pakistan.^{|||}Also at Key Laboratory of Nuclear Physics and Ion-beam Application (MOE) and Institute of Modern Physics, Fudan University, Shanghai 200443, People's Republic of China.

Published by the American Physical Society under the terms of the [Creative Commons Attribution 4.0 International license](https://creativecommons.org/licenses/by/4.0/). Further distribution of this work must maintain attribution to the author(s) and the published article's title, journal citation, and DOI. Funded by SCOAP³.

on the $\bar{K}\pi$ system. Furthermore, the form factors in the $D \rightarrow Ve^+\nu_e$ transition, where V refers to a vector meson, have been measured in decays of $D^+ \rightarrow \bar{K}^{*0}e^+\nu_e$ [4–6], $D \rightarrow \rho e^+\nu_e$ [7] and $D^+ \rightarrow \omega e^+\nu_e$ [8], while no form factor in $D^0 \rightarrow K^*(892)^-e^+\nu_e$ has been studied yet. Therefore, the study of the dynamics in the decay $D^0 \rightarrow K^*(892)^-e^+\nu_e$ provides essentially additional information on the family of $D \rightarrow Ve^+\nu_e$ decays.

In this paper, an improved measurement of the absolute branching fraction (BF) and the first measurement of the form factors of the decay $D^0 \rightarrow \bar{K}^0\pi^-e^+\nu_e$ are reported. These measurements are performed using an e^+e^- annihilation data sample corresponding to an integrated luminosity of 2.93 fb^{-1} produced at $\sqrt{s} = 3.773 \text{ GeV}$ with the BEPCII collider and collected with the BESIII detector [9].

II. BESIII DETECTOR AND MONTE CARLO SIMULATION

The BESIII detector is a cylindrical detector with a solid-angle coverage of 93% of 4π . The detector consists of a Helium-gas based main drift chamber (MDC), a plastic scintillator time-of-flight (TOF) system, a CsI(Tl) electromagnetic calorimeter (EMC), a superconducting solenoid providing a 1.0 T magnetic field and a muon counter. The charged particle momentum resolution is 0.5% at a transverse momentum of 1 GeV/ c . The photon energy resolution in EMC is 2.5% in the barrel and 5.0% in the end-caps at energies of 1 GeV. More details about the design and performance of the detector are given in Ref. [9].

A GEANT4-based [10] simulation package, which includes the geometric description of the detector and the detector response, is used to determine signal detection efficiencies and to estimate potential backgrounds. The production of the $\psi(3770)$, initial state radiation production of the $\psi(2S)$ and J/ψ , and the continuum processes $e^+e^- \rightarrow \tau^+\tau^-$ and $e^+e^- \rightarrow q\bar{q}$ ($q = u, d$ and s) are simulated with the event generator KKMC [11]. The known decay modes are generated by EVTGEN [12] with the branching fractions set to the world-average values from the Particle Data Group [13], while the remaining unknown decay modes are modeled by LUNDCHARM [14]. The generation of simulated signals $D^0 \rightarrow \bar{K}^0\pi^-e^+\nu_e$ incorporates knowledge of the form factors, which are obtained in this work.

III. ANALYSIS

The analysis makes use of both “single-tag” (ST) and “double-tag” (DT) samples of D decays. The single-tag sample is reconstructed in one of the final states listed in Table I, which are called the tag decay modes. Within each ST sample, a subset of events is selected where the other tracks in the event are consistent with the decay $D^0 \rightarrow \bar{K}^0\pi^-e^+\nu_e$. This subset is referred as the DT sample. For a specific tag mode i , the ST and DT event yields are expressed as

TABLE I. The selection requirements on ΔE , the signal region in the M_{BC} distribution, and the background-subtracted ST yields N_{ST} in data for each of the three tag decay modes.

Decay mode	ΔE (GeV)	Signal region (GeV/ c^2)	N_{ST} ($\times 10^3$)
$K^+\pi^-$	[-0.025, 0.028]	[1.860, 1.875]	540.2 ± 0.8
$K^+\pi^-\pi^-\pi^+$	[-0.020, 0.023]	[1.860, 1.875]	701.1 ± 1.7
$K^+\pi^-\pi^0$	[-0.044, 0.066]	[1.858, 1.875]	1035.9 ± 1.3

$$N_{\text{ST}}^i = 2N_{D^0\bar{D}^0}\mathcal{B}_{\text{ST}}^i\epsilon_{\text{ST}}^i, \quad N_{\text{DT}}^i = 2N_{D^0\bar{D}^0}\mathcal{B}_{\text{ST}}^i\mathcal{B}_{\text{SL}}\epsilon_{\text{DT}}^i,$$

where $N_{D^0\bar{D}^0}$ is the number of $D^0\bar{D}^0$ pairs, $\mathcal{B}_{\text{ST}}^i$ and \mathcal{B}_{SL} are the BFs of the \bar{D}^0 tag decay mode i and the D^0 SL decay mode, ϵ_{ST}^i is the efficiency for finding the tag candidate, and ϵ_{DT}^i is the efficiency for simultaneously finding the tag \bar{D}^0 and the SL decay. The BF for the SL decay is given by

$$\mathcal{B}_{\text{SL}} = \frac{N_{\text{DT}}}{\sum_i N_{\text{ST}}^i \times \epsilon_{\text{DT}}^i / \epsilon_{\text{ST}}^i} = \frac{N_{\text{DT}}}{N_{\text{ST}} \times \epsilon_{\text{SL}}}, \quad (1)$$

where N_{DT} is the total yield of DT events, N_{ST} is the total ST yield, and $\epsilon_{\text{SL}} = (\sum_i N_{\text{ST}}^i \times \epsilon_{\text{DT}}^i / \epsilon_{\text{ST}}^i) / \sum_i N_{\text{ST}}^i$ is the average efficiency of reconstructing the SL decay, weighted by the measured yields of tag modes in data.

Selection criteria for photons, charged pions and charged kaons are the same as those used in Ref. [15]. To reconstruct a π^0 candidate in the decay mode $\pi^0 \rightarrow \gamma\gamma$, the invariant mass of the candidate photon pair must be within (0.115, 0.150) GeV/ c^2 . To improve the momentum resolution, a kinematic fit is performed to constrain the $\gamma\gamma$ invariant mass to the nominal π^0 mass [13]. The χ^2 of this kinematic fit is required to be less than 20. The fitted π^0 momentum is used for reconstruction of the \bar{D}^0 tag candidates.

The ST \bar{D}^0 decays are identified using the beam constrained mass,

$$M_{\text{BC}} = \sqrt{(\sqrt{s}/2)^2 - |\vec{p}_{\bar{D}^0}|^2}, \quad (2)$$

where $\vec{p}_{\bar{D}^0}$ is the momentum of the \bar{D}^0 candidate in the rest frame of the initial e^+e^- system. To improve the purity of the tag decays, the energy difference $\Delta E = \sqrt{s}/2 - E_{\bar{D}^0}$ for each candidate is required to be within approximately $\pm 3\sigma_{\Delta E}$ around the fitted ΔE peak, where $\sigma_{\Delta E}$ is the ΔE resolution and $E_{\bar{D}^0}$ is the reconstructed \bar{D}^0 energy in the initial e^+e^- rest frame. The explicit ΔE requirements for the three ST modes are listed in Table I.

The distributions of the variable M_{BC} for the three ST modes are shown in Fig. 1. Maximum likelihood fits to the M_{BC} distributions are performed. The signal shape is derived from the convolution of the MC-simulated signal template function with a double-Gaussian function to

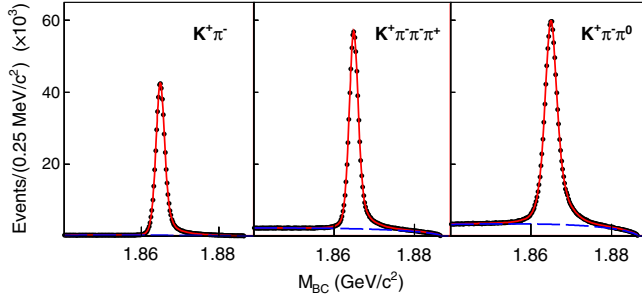


FIG. 1. The M_{BC} distributions for the three ST modes. The points are data, the (red) solid curves are the projection of the sum of all fit components and the (blue) dashed curves are the projection of the background component of the fit.

account for resolution difference between MC simulation and data. An ARGUS function [16] is used to describe the combinatorial background shape. For each tag mode, the ST yield is obtained by integrating the signal function over the D^0 signal region specified in Table I. In addition to the combinatorial background, there are also small wrong-sign (WS) peaking backgrounds in the ST \bar{D}^0 samples, which are from the doubly Cabibbo-suppressed decays of $\bar{D}^0 \rightarrow K^- \pi^+$, $K^- \pi^+ \pi^0$ and $K^- \pi^+ \pi^+ \pi^-$. The $\bar{D}^0 \rightarrow K_S^0 K^- \pi^+$, $K_S^0 \rightarrow \pi^+ \pi^-$ decay shares the same final states as the WS background of $\bar{D}^0 \rightarrow K^- \pi^+ \pi^+ \pi^-$. The sizes of these WS peaking backgrounds are estimated from simulation, and are subtracted from the corresponding ST yields. The background-subtracted ST yields are listed in Table I. The total ST yield summed over all three ST modes is $N_{ST} = (2277.2 \pm 2.3) \times 10^3$, where the uncertainty is statistical only.

Candidates for the SL decay $D^0 \rightarrow \bar{K}^0 \pi^- e^+ \nu_e$ are selected from the remaining tracks recoiling against the ST \bar{D}^0 mesons. The \bar{K}^0 meson is reconstructed as a K_S^0 . The K_S^0 mesons are reconstructed from two oppositely charged tracks and the invariant mass of the K_S^0 candidate is required to be within $(0.485, 0.510) \text{ GeV}/c^2$. For each K_S^0 candidate, a fit is applied to constrain the two charged tracks to a common vertex, and this K_S^0 decay vertex is required to be separated from the interaction point by more than twice the standard deviation of the measured flight distance. A further requirement is that there must only be two other tracks in the event and that they must be of opposite charge. The electron hypothesis is assigned to the track that has the same charge as that of the kaon on the tag side. For electron particle identification (PID), the specific ionization energy losses measured by the MDC, the time of flight, and the shower properties from the electromagnetic calorimeter (EMC) are used to construct likelihoods for electron, pion and kaon hypotheses (\mathcal{L}_e , \mathcal{L}_π and \mathcal{L}_K). The electron candidate must satisfy $\mathcal{L}_e > 0.001$ and $\mathcal{L}_e / (\mathcal{L}_e + \mathcal{L}_\pi + \mathcal{L}_K) > 0.8$. Additionally, the EMC energy of the electron candidate has to be more than 70% of the

track momentum measured in the MDC ($E/p > 0.7c$). The energy loss due to bremsstrahlung is partially recovered by adding the energy of the EMC showers that are within 5° of the electron direction and not matched to other particles [17]. The pion hypothesis is assigned to the remaining charged track and must satisfy the same criteria as in Ref. [15]. The background from $D^0 \rightarrow \bar{K}^0 \pi^+ \pi^-$ decays reconstructed as $D^0 \rightarrow \bar{K}^0 \pi^- e^+ \nu_e$ is rejected by requiring the $\bar{K}^0 \pi^- e^+$ invariant mass ($M_{\bar{K}^0 \pi^- e^+}$) to be less than $1.80 \text{ GeV}/c^2$. The backgrounds associated with fake photons are suppressed by requiring the maximum energy of any unused photon ($E_{\gamma_{\max}}$) to be less than 0.25 GeV.

The energy and momentum carried by the neutrino are denoted by E_{miss} and \vec{p}_{miss} , respectively. They are calculated from the energies and momenta of the tag ($E_{\bar{D}^0}$, $\vec{p}_{\bar{D}^0}$) and the measured SL decay products ($E_{\text{SL}} = E_{\bar{K}^0} + E_{\pi^-} + E_{e^+}$, $\vec{p}_{\text{SL}} = \vec{p}_{\bar{K}^0} + \vec{p}_{\pi^-} + \vec{p}_{e^+}$) using the relations $E_{\text{miss}} = \sqrt{s}/2 - E_{\text{SL}}$ and $\vec{p}_{\text{miss}} = \vec{p}_{\bar{D}^0} - \vec{p}_{\text{SL}}$ in the initial $e^+ e^-$ rest frame. Here, the momentum $\vec{p}_{\bar{D}^0}$ is given by $\vec{p}_{\bar{D}^0} = -\hat{p}_{\text{tag}} \sqrt{(\sqrt{s}/2)^2 - m_{\bar{D}^0}^2}$, where \hat{p}_{tag} is the momentum direction of the ST \bar{D}^0 and $m_{\bar{D}^0}$ is the nominal \bar{D}^0 mass [13]. Information on the undetected neutrino is obtained by using the variable U_{miss} defined by

$$U_{\text{miss}} \equiv E_{\text{miss}} - |\vec{p}_{\text{miss}}|. \quad (3)$$

The U_{miss} distribution is expected to peak at zero for signal events.

Figure 2(a) shows the U_{miss} distribution of the accepted candidate events for $D^0 \rightarrow \bar{K}^0 \pi^- e^+ \nu_e$ in data. To obtain the signal yield, an unbinned maximum likelihood fit of the U_{miss} distribution is performed. In the fit, the signal is described with a shape derived from the simulated signal events convolved with a Gaussian function, where the width of the Gaussian function is determined by the fit. The background is described by using the shape obtained from the MC simulation. The yield of DT $D^0 \rightarrow \bar{K}^0 \pi^- e^+ \nu_e$ events is determined to be $3131 \pm 64(\text{stat.})$. The backgrounds from the non- D^0 and non- K_S^0 decays are estimated by examining the ST candidates in the M_{BC} sideband, defined in the range $(1.830, 1.855) \text{ GeV}/c^2$, and the SL candidates in the K_S^0 sidebands, defined in the ranges $(0.450, 0.475) \text{ GeV}/c^2$ or $(0.525, 0.550) \text{ GeV}/c^2$ in data, respectively. The yield of this type of background is estimated to be 19.4 ± 5.3 . After subtracting these background events, we evaluate the number of the signal DT events to be $N_{\text{DT}} = 3112 \pm 64(\text{stat.})$.

The detection efficiency ε_{SL} is estimated to be $(9.53 \pm 0.01)\%$, and the BF of $D^0 \rightarrow \bar{K}^0 \pi^- e^+ \nu_e$ is determined as $\mathcal{B}(D^0 \rightarrow \bar{K}^0 \pi^- e^+ \nu_e) = (1.434 \pm 0.029(\text{stat.}))\%$. Due to the double tag technique, the BF measurement is insensitive to the systematic uncertainty in the ST efficiency. The uncertainties due to the pion and electron tracking efficiencies are estimated to be 0.5% [18] and the

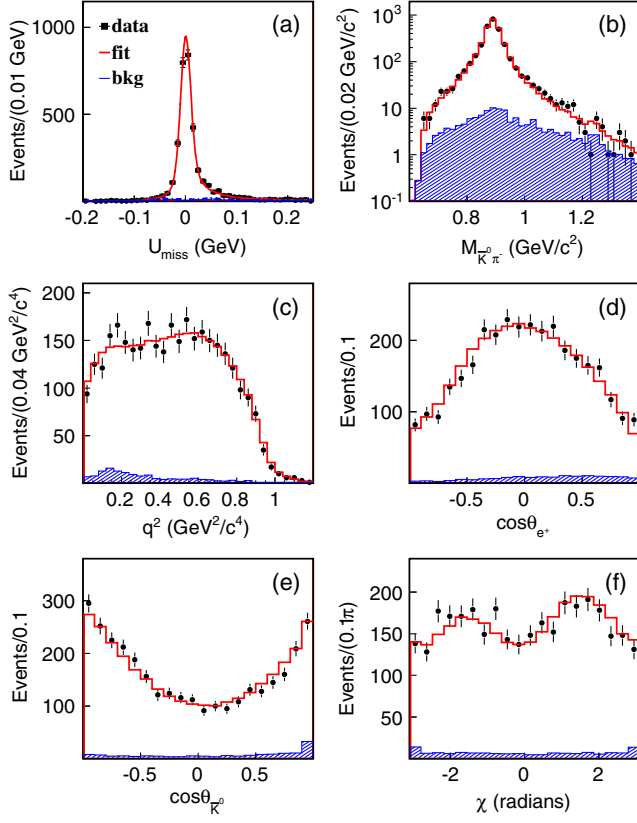


FIG. 2. (a) Fit to U_{miss} distribution of the SL candidate events. Projections onto five kinematic variables (b) $M_{\bar{K}^0\pi^-}$, (c) q^2 , (d) $\cos\theta_{e^+}$, (e) $\cos\theta_{\bar{K}^0}$, and (f) χ for $D^0 \rightarrow \bar{K}^0\pi^-e^+\nu_e$. The dots with error bars are data, the red curve/histograms are the fit results, and the shadowed histograms are the simulated background.

uncertainties due to their PID efficiencies are estimated to be 0.5% [18], where the tracking and PID uncertainties are conservatively estimated to account for the possible differences of the momentum spectra in Ref. [18]. The uncertainty due to the \bar{K}^0 reconstruction is 1.5% [15]. The uncertainty due to the E/p requirement is 0.4% [6]. The uncertainty associated with the $E_{\gamma\text{max}}$ requirement is estimated to be 0.4% by analyzing the DT $D^0\bar{D}^0$ events where both D mesons decay to hadronic final states. The uncertainty due to the modeling of the signal in simulated events is estimated to be 0.8% by varying the input form factor parameters by $\pm 1\sigma$ as determined in this work. The uncertainty associated with the fit of the U_{miss} distribution is estimated to be 0.7% by varying the fitting ranges and the shapes which parametrize the signal and background. The uncertainty associated with the fit of the M_{BC} distributions used to determine N_{ST} is 0.5% and is evaluated by varying the bin size, fit range and background distributions. Further systematic uncertainties are assigned due to the statistical precision of the simulation (0.2%), the background subtraction (0.2%), and the input BF of the decay $K_S^0 \rightarrow \pi^+\pi^-$ (0.1%). The systematic uncertainty contributions are

summed in quadrature, and the total systematic uncertainty on the BF measurement is 2.2% of the central value.

IV. $D^0 \rightarrow \bar{K}^0\pi^-e^+\nu_e$ DECAY RATE FORMALISM

The differential decay width of $D^0 \rightarrow \bar{K}^0\pi^-e^+\nu_e$ can be expressed in terms of five kinematic variables: the square of the invariant mass of the $\bar{K}^0\pi^-$ system $m_{\bar{K}^0\pi^-}^2$, the square of the invariant mass of the $e^+\nu_e$ system (q^2), the angle between the \bar{K}^0 and the D^0 direction in the $\bar{K}^0\pi^-$ rest frame ($\theta_{\bar{K}^0}$), the angle between the ν_e and the D^0 direction in the $e^+\nu_e$ rest frame (θ_e), and the acoplanarity angle between the two decay planes (χ). Neglecting the mass of e^+ , the differential decay width of $D^0 \rightarrow \bar{K}^0\pi^-e^+\nu_e$ can be expressed as [19]

$$d^5\Gamma = \frac{G_F^2 |V_{cs}|^2}{(4\pi)^6 m_{D^0}^3} X \beta \mathcal{I}(m_{\bar{K}^0\pi^-}^2, q^2, \theta_{\bar{K}^0}, \theta_e, \chi) dm_{\bar{K}^0\pi^-}^2 dq^2 d\cos\theta_{\bar{K}^0} d\cos\theta_e d\chi, \quad (4)$$

where $X = p_{\bar{K}^0\pi^-} m_{D^0}$, $\beta = 2p^*/m_{\bar{K}^0\pi^-}$, and $p_{\bar{K}^0\pi^-}$ is the momentum of the $\bar{K}^0\pi^-$ system in the rest D^0 system and p^* is the momentum of \bar{K}^0 in the $\bar{K}^0\pi^-$ rest frame. The Fermi coupling constant is denoted by G_F . The dependence of the decay density \mathcal{I} is given by

$$\begin{aligned} \mathcal{I} = & \mathcal{I}_1 + \mathcal{I}_2 \cos 2\theta_e + \mathcal{I}_3 \sin^2\theta_e \cos 2\chi + \mathcal{I}_4 \sin 2\theta_e \cos \chi \\ & + \mathcal{I}_5 \sin \theta_e \cos \chi + \mathcal{I}_6 \cos \theta_e + \mathcal{I}_7 \sin \theta_e \sin \chi \\ & + \mathcal{I}_8 \sin 2\theta_e \sin \chi + \mathcal{I}_9 \sin^2\theta_e \sin 2\chi, \end{aligned} \quad (5)$$

where $\mathcal{I}_{1,\dots,9}$ depend on $m_{\bar{K}^0\pi^-}^2$, q^2 and $\theta_{\bar{K}^0}$ [19] and can be expressed in terms of three form factors, $\mathcal{F}_{1,2,3}$. The form factors can be expanded into partial waves including S -wave (\mathcal{F}_{10}), P -wave (\mathcal{F}_{i1}) and D -wave (\mathcal{F}_{i2}), to show their explicit dependences on $\theta_{\bar{K}^0}$. Analyses of the decay $D^+ \rightarrow K^+\pi^-e^+\nu_e$ by using much higher statistics performed by the BABAR [5] and BESIII [6] collaborations do not observe a D -wave component and hence it is not considered in this analysis. Consequently, the form factors can be written as

$$\mathcal{F}_1 = \mathcal{F}_{10} + \mathcal{F}_{11} \cos\theta_{\bar{K}^0}, \quad \mathcal{F}_2 = \frac{1}{\sqrt{2}} \mathcal{F}_{21}, \quad \mathcal{F}_3 = \frac{1}{\sqrt{2}} \mathcal{F}_{31}, \quad (6)$$

where \mathcal{F}_{11} , \mathcal{F}_{21} and \mathcal{F}_{31} are related to the helicity basis form factors $H_{0,\pm}(q^2)$ [19,20]. The helicity form factors can in turn be related to the two axial-vector form factors, $A_1(q^2)$ and $A_2(q^2)$, as well as the vector form factor $V(q^2)$. The $A_{1,2}(q^2)$ and $V(q^2)$ are all taken as the simple pole form $A_i(q^2) = A_i(0)/(1 - q^2/M_A^2)$ and

$V(q^2) = V(0)/(1 - q^2/M_V^2)$, with pole masses $M_V = M_{D_s^*(1^-)} = 2.1121 \text{ GeV}/c^2$ [13] and $M_A = M_{D_s^*(1^+)} = 2.4595 \text{ GeV}/c^2$ [13]. The form factor $A_1(q^2)$ is common to all three helicity amplitudes. Therefore, it is natural to define two form factor ratios as $r_V = V(0)/A_1(0)$ and $r_2 = A_2(0)/A_1(0)$ at the momentum square $q^2 = 0$.

The amplitude of the P -wave resonance $\mathcal{A}(m)$ is expressed as [5,6]

$$\mathcal{A}(m) = \frac{m_0 \Gamma_0 (p^*/p_0^*)}{m_0^2 - m_{\bar{K}^0 \pi^-}^2 - im_0 \Gamma(m_{\bar{K}^0 \pi^-})} \frac{B(p^*)}{B(p_0^*)}, \quad (7)$$

where $B(p) = \frac{1}{\sqrt{1+R^2 p^2}}$ with $R = 3.07 \text{ GeV}^{-1}$ [6] and $\Gamma(m_{\bar{K}^0 \pi^-}) = \Gamma_0 \left(\frac{p_0^*}{p_0^*}\right)^3 \frac{m_0}{m_{\bar{K}^0 \pi^-}} \left[\frac{B(p^*)}{B(p_0^*)}\right]^2$, where p_0^* is the momentum of \bar{K}^0 at the pole mass of the resonance m_0 , and $\alpha = \sqrt{3\pi \mathcal{B}_{K^*} / (p_0^* \Gamma_0)}$, $\mathcal{B}_{K^*} = \mathcal{B}(K^*(892)^- \rightarrow \bar{K}^0 \pi^-)$.

The S -wave related \mathcal{F}_{10} is described by [5,6]

$$\mathcal{F}_{10} = p_{\bar{K}^0 \pi^-} m_{D^0} \frac{1}{1 - \frac{q^2}{m_A^2}} \mathcal{A}_S(m), \quad (8)$$

where the term $\mathcal{A}_S(m)$ corresponds to the mass-dependent S -wave amplitude, and the same expression of $\mathcal{A}_S(m) = r_S P(m) e^{i\delta_S(m)}$ as in Refs. [5,6] is adopted, in which $P(m) = 1 + x r_S^{(1)}$ with $x = \sqrt{\left(\frac{m}{m_{\bar{K}^0} + m_{\pi^-}}\right)^2 - 1}$, and $\delta_S(m) = \delta_{\text{BG}}^{1/2}$ with $\cot(\delta_{\text{BG}}^{1/2}) = 1/(a_{\text{S,BG}}^{1/2} p^*) + b_{\text{S,BG}}^{1/2} p^*/2$.

An unbinned five-dimensional maximum likelihood fit to the distributions of $m_{\bar{K}^0 \pi^-}$, q^2 , $\cos \theta_{e^+}$, $\cos \theta_{\bar{K}^0}$, and χ for the $D^0 \rightarrow \bar{K}^0 \pi^- e^+ \nu_e$ events within $-0.10 < U_{\text{miss}} < 0.15 \text{ GeV}$ is performed in a similar manner to Ref. [6]. The projected distributions of the fit onto the fitted variables are shown in Figs. 2(b–f). In this fit, the parameters of r_V , r_2 , m_0 , Γ_0 , r_S and $a_{\text{S,BG}}^{1/2}$ are float, while $r_S^{(1)}$ and $b_{\text{S,BG}}^{1/2}$ are fixed to 0.08 and $-0.81 \text{ (GeV}/c)^{-1}$ due to limited statistics, respectively, based on the analysis of $D^+ \rightarrow K^+ \pi^- e^+ \nu_e$ at BESIII [6]. The fit results are summarized in Table II. The goodness of fit is estimated

TABLE II. The fit results, where the first uncertainties are statistical and the second are systematic.

Variable	Value
$M_{K^*(892)^-} \text{ (MeV}/c^2)$	$891.7 \pm 0.6 \pm 0.2$
$\Gamma_{K^*(892)^-} \text{ (MeV)}$	$48.4 \pm 1.5 \pm 0.5$
$r_S \text{ (GeV)}^{-1}$	$-11.21 \pm 1.03 \pm 1.15$
$a_{\text{S,BG}}^{1/2} \text{ (GeV}/c)^{-1}$	$1.58 \pm 0.22 \pm 0.18$
r_V	$1.46 \pm 0.07 \pm 0.02$
r_2	$0.67 \pm 0.06 \pm 0.01$

by using the χ^2/ndof , where ndof denotes the number of degrees of freedom. The χ^2 is calculated from the comparison between the measured and expected number of events in the five-dimensional space of the kinematic variables $m_{\bar{K}^0 \pi^-}$, q^2 , $\cos \theta_{e^+}$, $\cos \theta_{\bar{K}^0}$, and χ which are initially divided into 2, 2, 3, 3, and 3 bins, respectively. The bins are set with different sizes, so that they contain sufficient numbers of signal events for credible χ^2 calculation. Each five-dimensional bin is required to contain at least ten events; otherwise, it is combined with an adjacent bin. The χ^2 value is calculated as

$$\chi^2 = \sum_i^{N_{\text{bin}}} \frac{(n_i^{\text{data}} - n_i^{\text{fit}})^2}{n_i^{\text{fit}}}, \quad (9)$$

where N_{bin} is the number of bins, n_i^{data} denotes the measured number of events of the i th bin, and n_i^{fit} denotes the expected number of events of the i th bin. The ndof is the number of bins minus the number of fit parameters minus 1. The χ^2/ndof obtained is 96.3/98, which shows a good fit quality. The fit procedure is validated using a large simulated sample of inclusive events, where the pull distribution of each fitted parameter is found to be consistent with a normal distribution.

The fit fraction of each component can be determined by the ratio of the decay intensity of the specific component and that of the total. The fractions of S -wave and P -wave ($K^*(892)^-$) are found to be $f_{S\text{-wave}} = (5.51 \pm 0.97(\text{stat.}))\%$ and $f_{K^*(892)^-} = (94.52 \pm 0.97(\text{stat.}))\%$, respectively.

The systematic uncertainties of the fitted parameters and the fractions of S -wave and $K^*(892)^-$ components are defined as the difference between the fit results in nominal conditions and those obtained after changing a variable or a condition by an amount which corresponds to an estimate of the uncertainty in the determination of this quantity. The systematic uncertainties due to the $E_{\gamma \text{max}}$ and E/p requirements are estimated by using alternative requirements of $E_{\gamma \text{max}} < 0.20 \text{ GeV}$ and $E/p > 0.75$, respectively. The systematic uncertainty because of the background fraction (f) is estimated by varying its value by $\pm 10\%$ which is the difference of the background fractions in the selected ST ΔE regions between data and MC simulation. The systematic uncertainties arising from the requirements placed on the charged pion, the electron and the K_S^0 are estimated by varying the pion/electron tracking and PID efficiencies, and K_S^0 detection efficiency by $\pm 0.5\%$, $\pm 0.5\%$ and $\pm 1.5\%$, respectively. The systematic uncertainty due to neglecting a possible contribution from the D -wave component is estimated by incorporating the D -wave component in Eq. (6). The systematic uncertainties in the fixed parameters of $r_S^{(1)}$ and $b_{\text{S,BG}}^{1/2}$ are estimated by varying their nominal values by $\pm 1\sigma$. All of the variations mentioned

TABLE III. Systematic uncertainties (in %) of the fitted parameters.

Parameter	$E_{\gamma\text{max}}$	E/p	f	Tracking&PID	D -wave	$r_S^{(1)}$	$b_{S,BG}^{1/2}$	Total
$M_{K^*(892)^-}$	0.00	0.01	0.00	0.00	0.01	0.01	0.01	0.02
$\Gamma_{K^*(892)^-}$	0.52	0.95	0.23	0.04	0.12	0.08	0.12	1.12
r_S	4.45	1.85	2.58	0.24	0.76	8.57	1.26	10.27
$a_{S,BG}^{1/2}$	7.66	3.52	1.36	0.26	0.87	0.11	7.78	11.59
r_V	0.34	0.83	0.37	0.57	0.12	0.29	0.42	1.21
r_2	0.95	0.27	0.30	0.02	0.27	0.03	0.60	1.22
$f_{K^*(892)^-}$	0.52	0.22	0.28	0.03	0.10	0.07	0.16	0.66
$f_{S\text{-wave}}$	8.89	3.81	4.72	0.54	1.81	1.09	2.54	11.27

above will result in differences of the fitted parameters and the extracted fractions of S -wave and $K^*(892)^-$ components from that under the nominal conditions. These differences are assigned as the systematic uncertainties and summarized in Table III, where the total systematic uncertainty is obtained by adding all contributions in quadrature.

V. SUMMARY

In summary, using 2.93 fb^{-1} of data collected at $\sqrt{s} = 3.773 \text{ GeV}$ by the BESIII detector, the absolute BF of $D^0 \rightarrow \bar{K}^0 \pi^- e^+ \nu_e$ is measured to be $\mathcal{B}(D^0 \rightarrow \bar{K}^0 \pi^- e^+ \nu_e) = (1.434 \pm 0.029(\text{stat.}) \pm 0.032(\text{syst.}))\%$, which is significantly more precise than the current world-average value [13]. The first analysis of the dynamics of $D^0 \rightarrow \bar{K}^0 \pi^- e^+ \nu_e$ decay is performed and the S -wave component is observed with a fraction $f_{S\text{-wave}} = (5.51 \pm 0.97(\text{stat.}) \pm 0.62(\text{syst.}))\%$, leading to $\mathcal{B}[D^0 \rightarrow (\bar{K}^0 \pi^-)_{S\text{-wave}} e^+ \nu_e] = (7.90 \pm 1.40(\text{stat.}) \pm 0.91(\text{syst.})) \times 10^{-4}$.

The P -wave component is observed with a fraction of $f_{K^*(892)^-} = (94.52 \pm 0.97(\text{stat.}) \pm 0.62(\text{syst.}))\%$ and the corresponding BF is given as $\mathcal{B}(D^0 \rightarrow K^*(892)^- e^+ \nu_e) = (2.033 \pm 0.046(\text{stat.}) \pm 0.047(\text{syst.}))\%$. It is consistent with, and more precise than, the result from the CLEO collaboration [21]. In addition, the form factor ratios of the $D^0 \rightarrow K^*(892)^- e^+ \nu_e$ decay are determined to be $r_V = 1.46 \pm 0.07(\text{stat.}) \pm 0.02(\text{syst.})$ and $r_2 = 0.67 \pm 0.06(\text{stat.}) \pm 0.01(\text{syst.})$. They are consistent with the measurements from the FOCUS collaboration [22] using the decay $D^0 \rightarrow \bar{K}^0 \pi^- \mu^+ \nu_\mu$ within uncertainties, but with significantly improved precision.

ACKNOWLEDGMENTS

The BESIII collaboration thanks the staff of BEPCII and the IHEP computing center for their strong support. This work is supported in part by National Key Basic Research Program of China under Contract No. 2015CB856700; National Natural Science Foundation of China (NSFC) under Contracts No. 11335008, No. 11425524, No. 11505010, No. 11625523, No. 11635010, No. 11735014, No. 11775027; the Chinese Academy of Sciences (CAS) Large-Scale Scientific Facility Program; the CAS Center for Excellence in Particle Physics (CCEPP); Joint Large-Scale Scientific Facility Funds of the NSFC and CAS under Contracts No. U1532257, No. U1532258, No. U1732263; CAS Key Research Program of Frontier Sciences under Contracts No. QYZDJ-SSW-SLH003, No. QYZDJ-SSW-SLH040; 100 Talents Program of CAS; Tsung-Dao Lee Institute and Shanghai Key Laboratory for Particle Physics and Cosmology; German Research Foundation DFG under Contracts Nos. Collaborative Research Center CRC 1044, FOR 2359; Istituto Nazionale di Fisica Nucleare, Italy; Koninklijke Nederlandse Akademie van Wetenschappen (KNAW) under Contract No. 530-4CDP03; Ministry of Development of Turkey under Contract No. DPT2006K-120470; National Science and Technology fund; The Swedish Research Council; U. S. Department of Energy under Contracts No. DE-FG02-05ER41374, No. DE-SC-0010118, No. DE-SC-0010504, No. DE-SC-0012069; University of Groningen (RuG) and the Helmholtzzentrum fuer Schwerionenforschung GmbH (GSI), Darmstadt. This paper is also supported by Beijing municipal government under Contract No. KM201610017009, No. 2015000020124G064, No. CIT&TCD201704047.

[1] M. Antonelli *et al.*, *Phys. Rep.* **494**, 197 (2010).

[2] N. Cabibbo, *Phys. Rev. Lett.* **10**, 531 (1963); M. Kobayashi and T. Maskawa, *Prog. Theor. Phys.* **49**, 652 (1973).

[3] Throughout this paper, mesons with no explicit charge denote either a charged or neutral meson; the charge-conjugate modes are implied, unless explicitly noted.

- [4] M. R. Shepherd *et al.* (CLEO Collaboration), *Phys. Rev. D* **74**, 052001 (2006); **81**, 112001 (2010).
- [5] P. del Amo Sanchez *et al.* (BABAR Collaboration), *Phys. Rev. D* **83**, 072001 (2011).
- [6] M. Ablikim *et al.* (BESIII Collaboration), *Phys. Rev. D* **94**, 032001 (2016).
- [7] S. Dobbs *et al.* (CLEO Collaboration), *Phys. Rev. Lett.* **110**, 131802 (2013).
- [8] M. Ablikim *et al.* (BESIII Collaboration), *Phys. Rev. D* **92**, 071101(R) (2015).
- [9] M. Ablikim *et al.* (BESIII Collaboration), *Nucl. Instrum. Methods Phys. Res., Sect. A* **614**, 345 (2010).
- [10] S. Agostinelli *et al.* (GEANT4 Collaboration), *Nucl. Instrum. Methods Phys. Res., Sect. A* **506**, 250 (2003).
- [11] S. Jadach, B. F. L. Ward, and Z. Was, *Comput. Phys. Commun.* **130**, 260 (2000); *Phys. Rev. D* **63**, 113009 (2001).
- [12] D. J. Lange, *Nucl. Instrum. Methods Phys. Res., Sect. A* **462**, 152 (2001); P. Rong-Gang, *Chin. Phys. C* **32**, 599 (2008).
- [13] M. Tanabashi *et al.* (Particle Data Group), *Phys. Rev. D* **98**, 030001 (2018).
- [14] J. C. Chen, G. S. Huang, X. R. Qi, D. H. Zhang, and Y. S. Zhu, *Phys. Rev. D* **62**, 034003 (2000).
- [15] M. Ablikim *et al.* (BESIII Collaboration), *Phys. Rev. Lett.* **118**, 112001 (2017).
- [16] H. Albrecht *et al.* (ARGUS Collaboration), *Phys. Lett. B* **241**, 278 (1990).
- [17] M. Ablikim *et al.* (BESIII Collaboration), *Phys. Rev. D* **92**, 112008 (2015); *Phys. Rev. Lett.* **115**, 221805 (2015).
- [18] M. Ablikim *et al.* (BESIII Collaboration), *Phys. Rev. D* **92**, 072012 (2015).
- [19] C. L. Y. Lee, M. Lu, and M. B. Wise, *Phys. Rev. D* **46**, 5040 (1992).
- [20] J. D. Richman and P. R. Burchat, *Rev. Mod. Phys.* **67**, 893 (1995).
- [21] T. E. Coan *et al.* (CLEO Collaboration), *Phys. Rev. Lett.* **95**, 181802 (2005).
- [22] J. M. Link *et al.* (FOCUS Collaboration), *Phys. Lett. B* **67**, 607 (2005).